Progress In Electromagnetics Research C, Vol. 21, 113–127, 2011

DESIGN AND IMPLEMENTATION OF AN X-BAND PULSED SOLID-STATE POWER AMPLIFIER WITH HIGH POWER AND HIGH EFFICIENCY USING RADIAL WAVEGUIDE COMBINER

H. Chen, X.-F. Ji, L.-J. Jiang, and Y.-X. Zhang

School of Electronic Engineering
University of Electronic Science and Technology of China
Chengdu 611731, China

Abstract—An X-band active radial-waveguide pulsed power amplifier (PA) with high power and high power added efficiency (PAE) is designed, fabricated, and measured in this paper. A bandwidth of 1000 MHz with peak power level of 53.2 dBm at the frequency 9.85 GHz, under the condition of 4 kHz pulse repeat frequency (PRF) and 10% of duty cycle, has been obtained by five-way radial waveguide power combiner. Key features of this combined device are its maximum PAE ($> 43.6\%$) and combining efficiency ($> 92.8\%$). From 9.5 to 10.5 GHz, the pulsed solid-state power amplifier (PSSPA) can provide a minimum output power level 51.4 dBm, which operates on the repeat frequency 4 kHz, duty cycle 10%. The gain varied between 41.4 and 43.1 dB at the desired frequency range, with only less than ± 0.9-dB gain variation, which displayed a flat gain ripple. The PAE of the active combiner fluctuated between 36.5% and 43.6% as frequency varied from 9.5 to 10.5 GHz.

1. INTRODUCTION

High power amplifiers (HPAs) are crucial in the design of modern Radar and wireless communication systems and, in particular, transmitter hardware. Power amplifiers (PAs) can generally be made to have high performance characteristics at low microwave frequencies, however, they are still limited in power and are difficult to design at higher microwave and millimeter-wave frequencies, forcing systems designers to use vacuum-tube devices. However, solid-state power

Received 5 March 2011, Accepted 14 April 2011, Scheduled 19 April 2011
Corresponding author: Hui Chen (hchen0730@yahoo.com.cn).

amplifiers (SSPAs) have many advantages over microwave tubes, including availability, reliability, graceful degradation and ease of maintenance [1–3]. Additionally, solid-state amplifiers are also capable of operating by low-voltage power supplies, suppressing need for high voltage modulators and eliminating possible X-ray emission [4, 5]. Therefore, this has motivated research activities in the area of spatial power combining or multiple solid-state amplifiers [6]. Many circuit-level combining approaches, such as corporate combining, suffer from increased loss (and, hence, reduced combining efficiency) as the number of devices increases. On the contrary, loss is relatively independent of the number of devices in a well-designed spatial combiner. As a result, the spatial power combining technique is favored in certain high-power applications requiring a large number of amplifiers [7].

The radial waveguide structure is widely used in array antennas, but little attention has been given to power divider/combiner [8–10]. In [10], the authors designed and implemented a broadband radial waveguide passive spatial combiner, and the electromagnetic modeling of this structure was developed. Until now, however, the active high-power combining system based on this structure has not been reported.

In this article, a high-power and high-efficiency PSSPA using radial waveguide divider-combiner circuit at X-band is designed, fabricated and measured. Using five high-power PA modules, the combined PSSPA produced 208.9 W peak power output and 43.6% maximal PAE at the frequency 9.85 GHz, under the condition of 4 kHz PRF and 10% of duty cycle. Within the band of interest (from 9.5 to 10.5 GHz), the gain varied between 41.4 and 43.1 dB, with less than ±0.9-dB gain variation.

2. CIRCUIT DESIGN

The designed PSSPA with high power and high PAE consists of a driving-stage HPA module, a five-way radial waveguide power divider, five combining-stage HPA modules, a five-way radial waveguide power combiner, and bias circuit. Therein, the HPA modules with high PAE and radial-waveguide power divider/combiner with low loss are very necessary to achieve the high-performance combining PSSPA, which will be illustrated below in details.

2.1. Operating Principle of the Combining Power Amplifier

According to the radial waveguide spatial power-combining idea, the general scheme of PSSPA with high power output is shown in Figure 1. The input RF (radio frequency) small signal is fed into the input

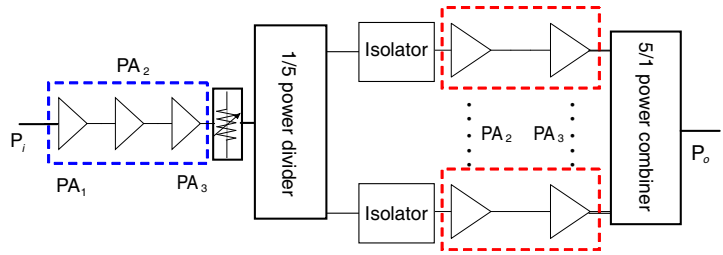

Figure 1. Schematic diagram of the SSPA using radial-waveguide structure.

port of the driving-stage HPA module, which consists of three-stage cascade PA units, i.e., PA_1, PA_2, and PA_3. A variable attenuator is followed after the driving module, whose main functionality is to tune the gain overall, so as to drive accurately the following the combining amplifier. To prevent the reflected high-power level from the divider/combiner into the PA modules, the low-loss and high-isolation microwave isolators (less than 0.2 dB and more than 25 dB in our design, respectively) are added to the input ports of each combining-stage PSSPA module, respectively. Finally, the amplified five-way pulsed power signals pour into the radial waveguide combiner synchronously by an equal-amplitude and in-phase means, offering a desired maximal power output.

2.2. Design of the HPA Modules

Based on the combing principle of the proposed SSPA in Section 2.1, two examples of cascade HPA for X-band based on hybrid MIC were designed, fabricated and measured, including the driving-stage and combining-stage PA modules. Firstly, some important considerations of the PA were taken and evaluated. Secondly, a three-stage cascade HPA and five two-stage cascade HPA modules for the pulse operation were designed and implemented, respectively. To obtain good characteristics, these PA units had been designed and evaluated separately before they were integrated together.

For a HPA design, especially at the microwave frequency band, there are some important factors considered, including the HPA devices and PCB grounding, DC blocking circuits, damping self-oscillation, and so on. At the initial stage of prototyping, the major constraints faced were insufficient power gain, low output power at P1 dB and oscillation. The reasons are provided and discussed in [11–22]. For the operating mode, class AB is selected in HPA modules. In our design,

the substrate used is the Rogers RT/Duroid 5880 with a thickness of 0.508 mm, dielectric loss tangent of 0.0009, and relative permittivity, ε_r of 2.2.

In the driving-stage design, the X-band HPA module consists of three amplification units, including MMIC HPA_1, HPA_2, and HPA_3. The HPA_2 is cascaded after the MMIC HPA_1, and the HPA_3 is cascaded after HPA_2. The HPA_1 is an internally matched MMIC amplifier that contains a three-stage amplifier, which has a typical linear gain of 27 dB and output P1 dB of 33 dBm, while the HPA_2 and HPA_3 are a power GaAs FET that is internally matched for standard communication bands to provide optimum power and gain in a 50 Ω system. The three power devices are hermetically sealed package and internally matched to 50 ohm at the input and output. Similarly, the combining-stage HPA module makes up of HPA_2 and HPA_3, which are same as the driving-stage module. Figure 2 shows the operational scheme of the pulsed HPA modules. For the driving stage, the cascade pulsed HPA is shown in Figure 2(a), which can be realized by switching the supply voltage of the active devices. The amplified driving signal is again fed into the input port of the five-way radial waveguide power divider, whose output signals are then fed into each input port of five-way combing-stage HPA modules shown in Figure 2(b), respectively. This pulsed amplifier has a high efficiency and low noise floor level

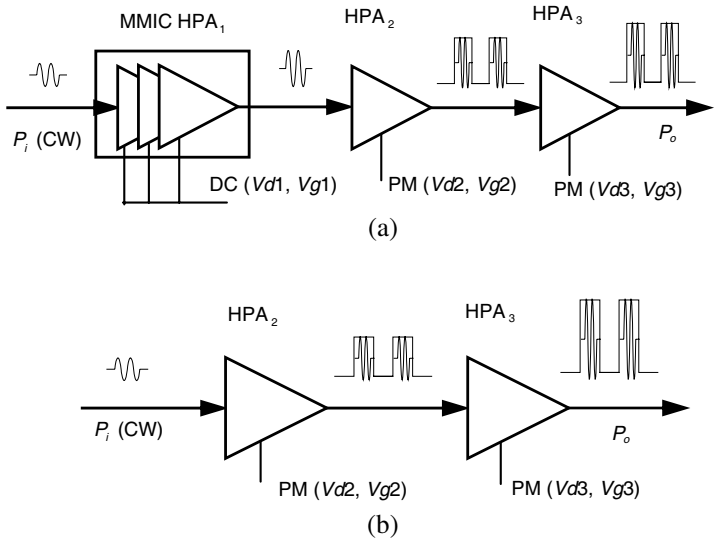

Figure 2. Schematic block diagram of the X-band pulsed HPA modules. (a) Driving-stage HPA module. (b) Combining-stage HPA module.

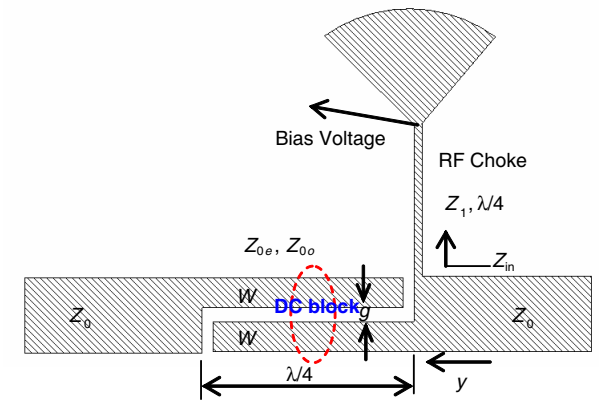

Figure 3. Biasing circuit using multisections shunt stubs for large bandwidths: A combination of $\lambda/4$ section and radial line configuration.

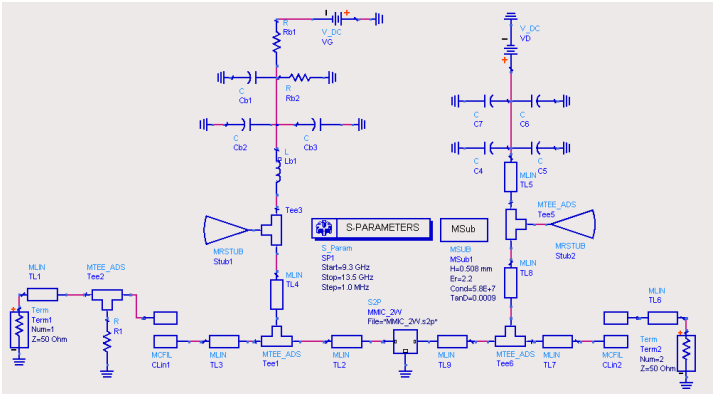

Figure 4. ADS small signal model of the HPA_1 at the driving-stage module.

because of supplying bias voltage only for high level of pulse.

Based on the earlier design considerations of the HPA, the completed cascade PA module was designed by the DC block and bias circuit shown in Figure 3. In Figure 4, the Agilent ADS small signal model of designed MMIC HPA_1 is shown. The simulated results validated the original DC bias idea. The optimized SSPA module was enclosed with screws. The photographs of the fabricated HPAs are shown in Figures 5 and 6 (Removing the top cover of the installation housing), respectively.

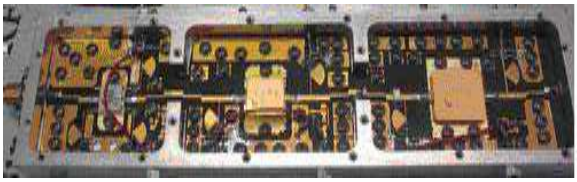

Figure 5. Photograph of the driving-stage HPA module.

Figure 6. Photograph of the combining-stage HPA module.

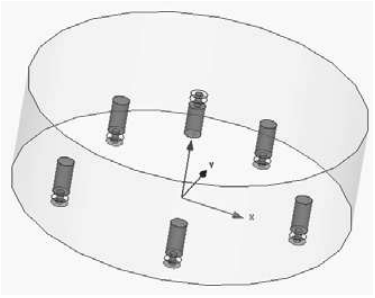

(a)

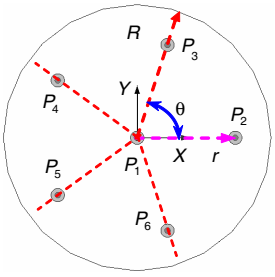

(b)

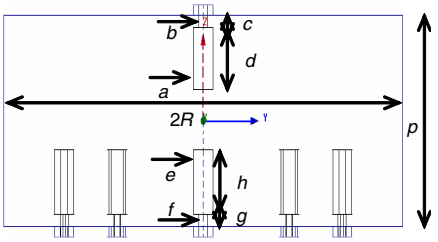

(c)

Figure 7. Schematic views of five-way radial waveguide power divider/combiner. (a) Three-dimensional view. (b) Top view. (c) Front view.

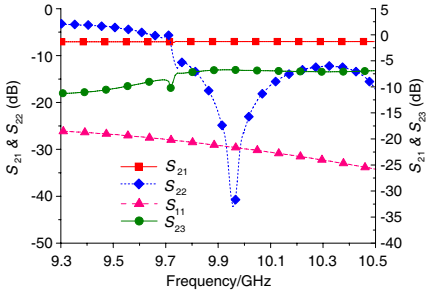

Figure 8. Simulated frequency responses of the five-way power divider/combiner.

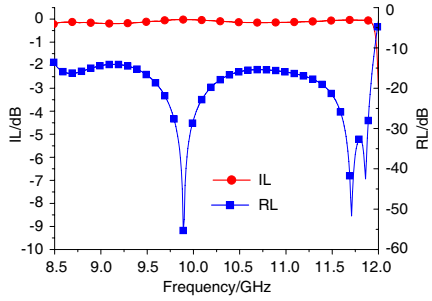

Figure 9. S-parameter characteristics of the passive combined system.

2.3. Design of a Five-way Power Divider/Combiner

Figure 7 shows the configurable views of the radial waveguide power divider/combiner. This radial waveguide power divider consists of a central coaxial probe in the radial waveguide and five symmetrically located peripheral coaxial probes. The input power from central probe port P_1 is divided five ways using five equispaced identical peripheral probes (port numbers shown in Figure 7(b) are noted P_2, P_3, P_4, P_5, P_6, respectively.). A short wall placed beyond the probe presents an open circuit to the probe. As a result, it is possible for the divider to divide an input power equally with no reflection loss at the input port, and to combine five-way equal-amplitude and in-phase inputs completely. The operation frequency and bandwidth is determined by the probe dimensions and the electrical length between the waveguide short wall and the center of probe array.

Based on the design method demonstrated clearly in [10] and [23, 24], a five-way radial waveguide power divider/combiner was designed. The initial dimensions of the circuit as illustrated in Figure 7 were as follows: radial cavity diameter $2R = 60.0\,\text{mm}$, height $p = 20.0\,\text{mm}$, and location of the peripheral coaxial probes $r = 22.0\,\text{mm}$ from the cavity centre. The central probe dimensions were as follows: disc diameter $a = 3.0\,\text{mm}$, disc height $d = 5.3\,\text{mm}$, coaxial probe inner conductor diameter $b = 1.3\,\text{mm}$, outer conductor diameter 4.2 mm, and height between the waveguide floor and the disc $c = 2.2\,\text{mm}$. The peripheral probe dimensions were as follows: disc diameter $e = 2.4\,\text{mm}$, disc height $h = 6.5\,\text{mm}$, and the coaxial probe dimensions are the same as those of coaxial probe described earlier, that is, $f = 1.3\,\text{mm}$, $g = 2.2\,\text{mm}$. The power divider/combiner is terminated by commercially available type-SMA connectors.

The designed circuit was simulated and optimized by full-wave electromagnetic (EM) simulator HFSS. The finally obtained S parameters are presented in Figure 8. From 9.3 to 10.5 GHz, the simulated transmission coefficient, S_{21}, is better than -7.1 dB, and input return loss, S_{11}, more than 18.5 dB. The output return loss, S_{22}, is more than 10.5 dB from 9.73 to 10.5 GHz. The isolation between output ports, S_{23}, is more than 6.8 dB from 9.3 to 10.5 GHz. Specially, this value is more than 8 dB from 9.3 to 9.73 GHz.

A passive spatial combiner was built by placing two identical power-dividing circuits [see Figure 7(a)] back to back. Figure 9 shows the simulated insertion and return losses for the passive spatial combiner. It showed that the return loss was more than 15 dB from 8.5 to 12 GHz, and its insertion loss is found to be less than 0.2 from 8.5 to 11.8 GHz. According to the design results above, two identical waveguide circuits were fabricated and assembled, and the photographs are shown in Figure 10.

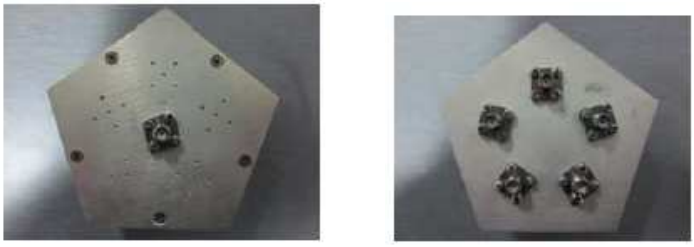

(a) (b)

Figure 10. Photographs of the five-way power divider/combiner. (a) Top view. (b) Bottom view.

3. EXPERIMENTAL RESULTS

Based on the design concepts discussed above, each part of the power-combined amplifier was fabricated and tuned independently. Finally, all parts were again assembled together. To verify the validity of the power-combined idea described in Section 2.1, the experiments on the designed power-combined circuit were performed. The measured results are demonstrated below.

3.1. Results of the HPA Modules

The measurements on the HPA module were divided into two types, that is, one of driving-stage amplifier module shown in Figure 5,

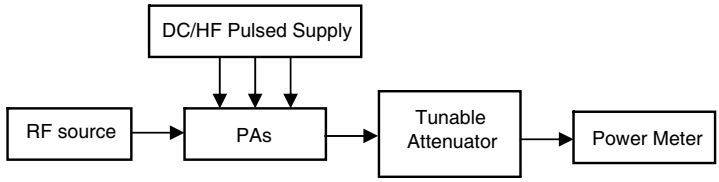

Figure 11. Test scheme of the driving-stage pulsed HPA module.

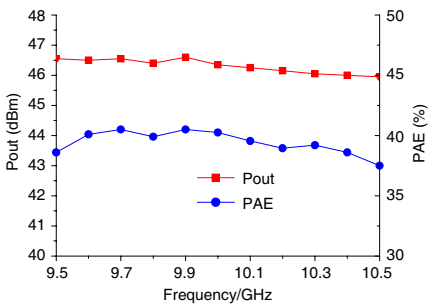

Figure 12. Pout and PAE versus frequency of the cascade HPA with 10 dBm input power.

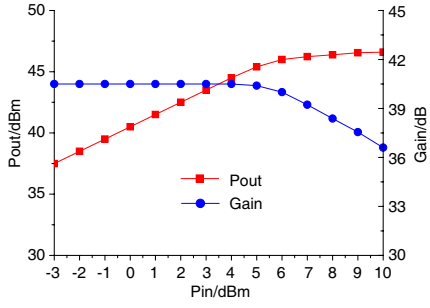

Figure 13. Output power and gain as functions of input power for the three-stage cascade HPA module at 9.9 GHz under pulse mode.

and another of combining-stage amplifier module shown in Figure 6. Figure 11 shows the test principle of the driving-stage module. The DC bias conditions for the first-stage HPA_1 [see also Figure 2(a)] are $Vd1 = 6.5\,\text{V}$, $Vg1 = -5\,\text{V}$, while the middle-stage HPA_2 and final-stage HPA_3 are biased by HF (high frequency) switch supply at $Vd2 = Vd3 = 10\,\text{V}$, $Vg2 = Vg3 = -3\,\text{V}$ under the condition of 4 kHz PRF and 10% of duty cycle. The output power, Pout, and PAE as functions of frequency are shown in Figure 12. From 9.5 to 10.5 GHz, the pulsed output power ranges between 45.8 and 46.6 dBm, and the PAE varies between 35.8% and 40.5%, with a 10 dBm input power. The output power and gain as a function of input power measured at 9.9 GHz are shown in Figure 13. It can be observed that the saturated output power is as large as 46.6 dBm (45 W).

3.2. Results of the Five-way Power Divider/Combiner

According to the design principle discussed in Section 2.3, the five-way power divider/combiner was implemented and measured, as shown

Figure 14. Five-way divider/combiner measurement setup.

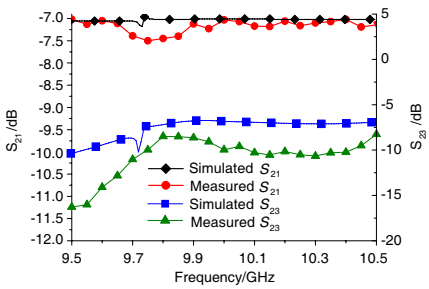

Figure 15. Simulated and measured transmission loss and isolation between the adjacent output ports for five-way power divider/combiner.

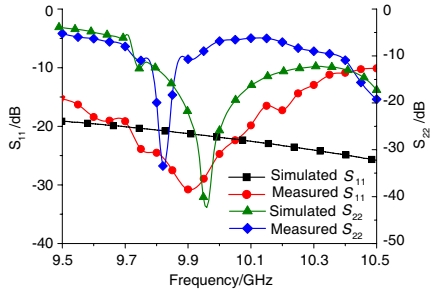

Figure 16. Simulated and measured return losses for five-way power divider/combiner at input and output ports, respectively.

in Figure 14. The simulated and measured results for the radial waveguide power divider/combiner are presented in Figures 15 and 16, respectively.

Figure 15 shows the simulated and measured transmission loss and isolation between the adjacent output ports, which displays that the measured response is an essential agreement with the simulated results from 9.5 to 10.5 GHz. The measured transmission coefficient, S_{21}, is better than -7.5 dB at our frequency range of interest. Compared with the simulation results, the increased insertion loss is most likely attributed to the fabrication errors such as inaccuracies in assembling the coaxial probes and SMA connectors. The measured isolation, S_{23}, is more than 8.5 dB from 9.5 to 10.5 GHz, whose result is better than the simulated one. In Figure 16, the return losses of input and output ports are also displayed. Obviously, the measured results are

an essential agreement with the simulated ones from 9.5 to 10.5 GHz. Over the desired frequency band, the measured return loss at input port, S_{11}, is more than 10.2 dB, while the one at output port, S_{22}, is more than 5.3 dB. Moreover, the imbalances of the phase/amplitude among the 5-way signal ports were also measured. For the fabricated divider/combiner, the imbalance of amplitude is less than ± 0.25 dB, and the one of phase is less than $\pm 3.6°$. Obviously, the designed power divider/combiner have shown a good phase/amplitude consistency in our interesting frequency range.

In addition, the passive power combiner assembled by placing two identical power-dividing circuits back to back was also measured. Figure 17 shows the simulated and measured responses over the frequency range from 9.5 to 10.5 GHz. Once more, a good agreement between the measured results with simulated ones was achieved. It showed that the return loss was more than 7.2 dB, while its insertion loss less than 0.36 dB from 9.5 to 10.5 GHz.

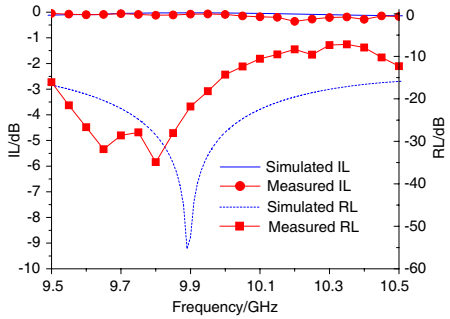

Figure 17. Simulated and measured results of the passive back-to-back circuit for five-way power divider/combiner.

3.3. Results of the Combined PSSPA

Based on the experiments performed on Section 3.1 and 3.2, the assembled PSSPA was measured ultimately. Figure 18 shows the setup for the power measurement. Prior to the measurements, a calibration procedure was performed with extra care so that the RF power level at the output port of the combiner circuit could be directly determined based on the readings from power meter.

The power measurement results for the five-way power combiner with Pin = 10 dBm, under the pulse condition of 4 kHz PRF and 10% of duty cycle, are shown in Figure 19. A maximum output power of 208.9 W (53.2 dBm) was observed at the frequency 9.85 GHz, with a

corresponding gain more than 42.8 dB and PAE in excess of 43.5%. The gain varied between 41.4–43.1 dB from 9.5 to 10.5 GHz, with only less than ±0.9-dB gain variation, which displayed a flat gain ripple. Within the band of interest, the minimum output power is greater than 138 W (51.4 dBm), and the maximum combining efficiency is more than 92.8%. The PAE of the combiner circuit fluctuated between 36.5% and 43.6% as frequency varied from 9.5 to 10.5 GHz. As the MMIC HPA_1 in driving-stage PA module shown in Figure 2(a) is biased by DC supply, while the 5 HPA_2s and 5 HPA_3s in combining-stage HPA modules shown in Figure 2(b) are biased by HF switch supply, as a result, the over system's PAE is slightly better than the driving-stage PA module's one. By the way, the PAE of combined PA would be improved properly, if the MMIC HPA_1 at the driving-stage HPA

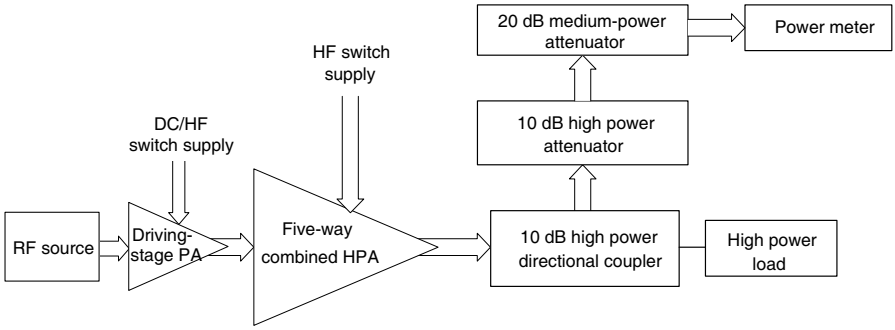

Figure 18. Power-combined PSSPA measurement setup.

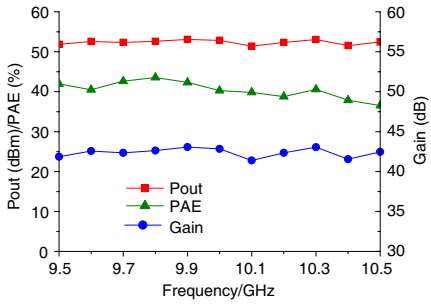

Figure 19. Power measurement results for power-combined PSSPA at Pin = 10 dBm, $Vd1$ = 6.5 V, $Vg1 = -5$ V, and $Vd2 = Vd3 = 10$ V, $Vg2 = Vg3 = -3$ V.

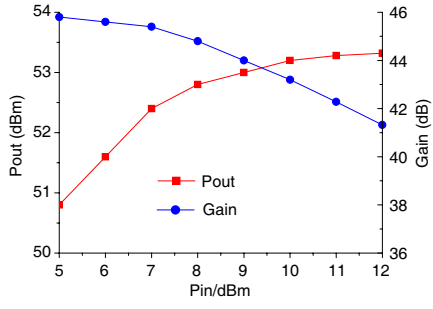

Figure 20. Pout, and gain versus Pin near saturation for power-combined PSSPA at 9.85 GHz.

module was also biased by HF switch supply.

Figure 20 shows output power versus input power for the combiner at 9.85 GHz, under the condition of 4 kHz PRF and 10% of duty cycle. The combining-stage HPA modules were biased by HF switch supply at $Vd = 10\,\text{V}$, $Vg = -3\,\text{V}$, and the input power sweep was focused around the range near saturation. As a result, it was found that the measurement of a full power sweep couldn't be well into the linear gain region, and the gain declined sharply as the input power level increased.

4. CONCLUSION

A five-way radial waveguide active spatial combiner with high power and high PAE has been demonstrated in this paper. A maximum output power of 208.9 W (pulsed peak power) was observed at 9.85 GHz, with a corresponding gain more than 42.8 dB and PAE in excess of 43.5%. The gain varied between 41.4 and 43.1 dB from 9.5 to 10.5 GHz, with only lower than ± 0.9-dB gain variation, which displayed good gain flatness. In addition, the PAE of the active combiner fluctuated between 36.5% and 43.6% as frequency varied from 9.5 to 10.5 GHz.

The hybrid-circuit approach also allows RF/microwave circuit engineers the flexibility of choosing active devices based on different technologies, thanks to the modular design of the combiner circuit, enabling easy maintenance, variable output power level, and potential medium-scale fabrication. It is worth mentioning that higher RF power output is possible achieved, which can use more than five-way waveguide combiner and higher power PA modules.

ACKNOWLEDGMENT

This work was supported in part by the China Postdoctoral Science Foundation (No. 20100471665), and in part by the National Natural Science Foundation of China (No. 60901020).

REFERENCES

1. Gregers-Hansen, V., "Radar systems trade-offs, vacuum electronics vs. solid-state," *Proc. 5th IEEE Inter. Conf. Vacuum Electronics*, 12–13, Apr. 2004.
2. Giacomo, M. D., "Solid-state RF amplifiers for accelerator applications," *Proc. Particle Accelerator Conf.*, May 2009.

3. Symons, R. S., "Modern microwave power sources," *IEEE AESS Systems Magazine*, Vol. 17, 19–26, Jan. 2002.
4. Koryu Ishii, T., *Microwave Technology: Components and Devices, (Handbook Style)*, Academic Press Inc., 1995.
5. Schirmer, A., "Emission of parasitic X-rays from military radar transmitters and exposure of personnel: Towards a retrospective assessment," *Proc. 2nd European IRPA Cong. Radiation Protection*, Paris, May 2006.
6. Gouker, M. A., "Spatial power combining," *Active and Quasi-optical Arrays for Solid-state Power Combining*, R. A. York and Z. B. Popovic (eds.), Wiley, New York, 1997.
7. Cheng, N. S., T. P. Dao, M. G. Case, D. B. Rensch, and R. A. York, "A 120-wattX-band spatially combined solid state amplifier," *IEEE Trans. Mircow. Theory Tech.*, Vol. 47, No. 12, 2557–2561, Dec. 1999.
8. Bialkowski, M. E. and V. P. Waris, "Electromagnetic model of a planar radial-waveguide divider/combiner incorporating probes," *IEEE Trans. Microw. Theory Tech.*, Vol. 41, Nos. 6–7, 1126–1134, Jun. 1993.
9. Schellenberg, J. and M. Cohn, "A wideband radial power combiner for FET amplifiers," *IEEE ISSC Int. Dig.*, 164–165, 1978.
10. Song, K. J., Y. Fan, and Z. R. He, "Broadband radial waveguide spatial combiner," *IEEE Microwave and Wireless Components Letters*, Vol. 18, No. 2, 73–75, Feb. 2008.
11. Gilmore, R. and L. Besser, *Practical RF Circuit Design for Modern Wireless Systems (Volume II)*, Artech House, Norwood, MA, 2003.
12. Sayre, C. W., *Complete Wireless Design*, 2nd edition, McGraw-Hill, 2008.
13. Lacombe, D. and J. Cohen, "Octave-band microstrip DC blocks," *IEEE Trans. Microwave Technology Tech.*, Vol. 20, 555–556, Aug. 1972.
14. Ho, C. Y., "Analysis of DC blocks using coupled lines," *IEEE Trans. Microwave Technology Tech.*, Vol. 23, 773–774, Sep. 1975.
15. Kajfez, D. and B. S. Vidula, "Design equations for symmetric microstrip DC blocks," *IEEE Trans. Microwave Technology Tech.*, Vol. 28, 974–981, Sep. 1980.
16. Dixon, P., "Dampening cavity resonance using absorber material," *RF Design Magazine*, 16–19, May 2004.
17. Syrett, B. A., "A broadband element for microstrip bias or tuning circuits," *IEEE Trans. MTT*, Vol. 28, No. 8, 488–491, Aug. 1980.

18. Basset, R., "High power GaAs FET device bias considerations," Fujitsu Compound Semiconductor, Inc., Application Note, No. 010, http://www.fcsi.fujitsu.com/.
19. Zhang, B., Y.-Z. Xiong, L. Wang, S. Hu, T.-G. Lim, Y.-Q. Zhuang, and L.-W. Li, "A D-band power amplifier with 30-GHz bandwidth and 4.5-dBm psat for high-speed communication system," *Progress In Electromagnetics Research*, Vol. 107, 161–178, 2010.
20. Mandeep, J. S., A. Lokesh, S. I. S. Hassan, M. N. Mahmud, and M. F. Ain, "Design of cartesian feedback RF power amplifier for L-band frequency range," *Progress In Electromagnetics Research B*, Vol. 2, 207–222, 2008.
21. Jiménez-Martín, J. L., V. Gonzalez-Posadas, J. E. Gonzalez-Garcia, F. J. Arques-Orobon, L. E. Garcia-Munoz, and D. Segovia-Vargas, "Dual band high efficiency class CE power amplifier based on CRLH diplexer," *Progress In Electromagnetics Research*, Vol. 97, 217–240, 2009.
22. Lee, M.-W., S.-H. Kam, Y.-S. Lee, and Y.-H. Jeong, "A highly efficient three-stage Doherty power amplifier with flat gain for WCDMA applications," *Journal of Electromagnetic Waves and Applications*, Vol. 24, No. 17–18, 2537–2545, 2010.
23. Bialkowski, M. E. and V. P. Waristt, "A systematic approach to the design of radial-waveguide dividers/combiners," *Asia-pacific Microwave Conference*, 881–884, 1992.
24. Fathy, A. E., S.-W. Lee, and D. Kalokitis, "A simplified design approach for radial power combiners," *IEEE Trans. on MTT.*, Vol. 54, No. 1, 247–255, Jan. 2006.